KBr@YAG:Ce^{3+} PHOSPHOR COMPOUND AIMING TO THE OPTICAL IMPROVEMENTS WHITE LEDS

Le Thi Trang[1], *Nguyen Van Dung*[2,*]

[1]Faculty of Information Technology, Dong Nai Technology University, Bien Hoa City, Vietnam.
[2]Faculty of Engineering, Dong Nai Technology University, Bien Hoa City, Vietnam.

*Corresponding Author: Nguyen Van Dung (Email: nguyenvandung@dntu.edu.vn)
(Received: 05-February-2025; accepted: 26-May-2025; published: 30-June-2025)
http://dx.doi.org/10.55579/jaec.202592.486

Abstract. *This study presents the utilization of KBr phosphor powder and its simulation works in conventional phosphor compound for improving the luminescence and color uniformity of the white light-emitted diodes (WLED) light output. The introduction of KBr powder with a radius of 4 microns may result in the scattering of the phosphor compound, contributing to the better wide-angle light dispersion performance. The simulation of KBr is carried out with Mie-Lorenz scattering practices and MATLAB programs. The concentration of KBr powder in the phosphor compound is adjusted to gauge its influence on various optical attributes such as scattering coefficient, YGA:Ce^{3+} phosphor dosage, angular distribution of light, etc. Results demonstrate that the increase of scattering strength and variation color variation under larger KBr powder concentration. The increase in lumen output is noted under higher concentration of KBr in the compound while the chromatic rendition performance, expressed via CRI and CQS, is preserved. The findings show that there is potential in using KBr powder for improving the performance of phosphor compound under visible excitation wavelengths.*

Key Words: *WLED; KBr; color deviation; light scatters; luminescence properties.*

1. Introduction

White light-emitted diodes (WLEDs) represent a transformative advancement in lighting technology, significantly enhancing human vision and overall quality of life. This advancement is driven by the efficiency, affordability, and practicality of LEDs, coupled with their vast potential for customization of spectral power distribution. As such, WLEDs are employed for diverse lighting applications, from everyday household illumination to sophisticated environments such as museums and digital displays.

Regarding the development of WLEDs, the phosphor conversion technique is favored over the combination of multiple LEDs to achieve the desired spectral power distribution [1, 2]. This approach typically involves using various phosphors, such as the widely-used yellow YAG:Ce^{3+}, in conjunction with one or more blue LED chips to generate white light. Despite the tunability of emission and correlated color temperature (CCT), phosphor-conversion WLEDs face energy losses due to phosphor absorption, which is converted to heat [3, 4]. This heat is difficult to dissipate and negatively impacts the reliability and performance of the LEDs [5, 6].

To address these challenges, recent advancements have focused on enhancing the light performance of phosphor-converted WLEDs [7, 8].

One promising strategy involves modifying phosphor compounds by incorporating particles with high transmittance indices, compatible refractive indices, or unique scattering properties [9, 10]. Commonly investigated particles include SiO_2, TiO_2, and ZnO. Additionally, KBr has emerged as a promising material for improving light transmission efficiency in WLEDs. Known for its high transparency across a wide range of wavelengths, from the ultraviolet to the far infrared, KBr exhibits low absorption and a low refractive index, ensuring high theoretical transmission without requiring anti-reflective coatings. Furthermore, KBr is cost-effective and non-toxic, making it ideal for economical production. However, in powder form, KBr's transmission efficiency is reduced due to absorption and scattering at particle boundaries. Compared to earlier studies by Thi et al. on Eu^{2+}-activated strontium-barium silicate, and That and Anh on green $Ca_2La_2BO_{6.5}$:Pb^{2+} phosphor, the KBr phosphor in this study has a more consistent effect on scattering coefficient and shows a noticeably greater ability to maintain lumen and color rendition.

This study investigates the incorporation of KBr powder into YAG:Ce^{3+} phosphor compounds. The Mie-Lorenz simulation is used to demonstrate the effects of different KBr concentrations on the light performance of the phosphor compound. Mie-scattering-based software and MATLAB programs, scattering simulations are employed for analyzing these effects. Section 2. details the computational models used for the simulations, followed by a discussion of the results in Section 3. Finally, the paper concludes with a summary in Section 4.

2. Scattering Simulation

The mathematical models of scattering in the simulation utilize the Mie-scattering hypothesis and are demonstrated with MATLAB program. The scattering coefficient $\mu_{\text{sca}}(\lambda)$ is the mean of measuring the scattering factor of the phosphor composite in this work. The following expressions are employed to determine $\mu_{\text{sca}}(\lambda)$ [11,12]:

$$\mu_{sca}(\lambda) = \int N(r) C_{sca}(\lambda, r)\, dr \tag{1}$$

$$C_{sca} = \frac{2\pi}{k^2} \sum_{n=0}^{\infty} (2n-1) \left(|a_n|^2 + |b_n|^2 \right) \tag{2}$$

where $N(r)$ and C_{sca} indicate the particle's distribution density and the scattering cross section, respectively; λ and r signify the wavelength and particle size, respectively. With the scattering cross-section, a_n and b_n can be computed as follows [13,14]:

$$a_n(x,m) = \frac{\psi_n'(mx)\psi_n(x) - m\psi_n(mx)\psi_n'(x)}{\psi_n'(mx)\xi_n(x) - m\psi_n(mx)\xi_n'(x)} \tag{3}$$

$$b_n(x,m) = \frac{m\psi_n'(mx)\psi_n(x) - \psi_n(mx)\psi_n'(x)}{m\psi_n'(mx)\xi_n(x) - \psi_n(mx)\xi_n'(x)} \tag{4}$$

where $k = 2\pi/\lambda$ and $x = kr$; m indicates the refractive index; $\psi_n(x)$ and $\xi_n(x)$ are the Riccati-Bessel functions. The particle distributing density $N(r)$ is the sum of the densities of the KBr and phosphor particles, signified by $N_{dif}(r)$ and $N_{phos}(r)$, respectively, which are expressed as follows [15,16]:

$$N(r) = N_{dif}(r) + N_{phos}(r) = K_N \left[f_{dif}(r) + f_{phos}(r) \right] \tag{5}$$

where K_N is the number of diffusor units or KBr particles; $f_{dif}(r)$ and $f_{phos}(r)$ denote the size distribution function data of the KBr and phosphor particles.

Using K_N, the diffusor concentration can be computed as [17,18]:

$$c = K_N \int M(r)\, dr \tag{6}$$

where $M(r)$ is the mass distribution of the diffusive unit, determined by the following equation [19,20]:

$$M(r) = \frac{4}{3}\pi r^3 \left[\rho_{dif} f_{dif}(r) + \rho_{phos} f_{phos}(r) \right] \tag{7}$$

where the diffusor and phosphor crystal densities are $\rho_{dif}(r)$ and $\rho_{phos}(r)$, respectively.
These mathematical models assess the scattering processes for different concentrations of KBr while maintaining a constant particle size of 4 microns. The simulation is conducted with KBr concentrations varying from 5 wt% to 9 wt%. Theoretically, the increase in KBr amount will improve the scattering coefficients owing to the denser particle distribution [21,22]. The greater

scattering will benefit the color distribution uniformity in general [23, 24]. To validate these hypotheses, the simulation work and the results are presented and discussed in the next section.

3. Result and Discussion

The scattering coefficients monitored under different KBr amounts are presented in Figure 1. When heightening the doping concentration of KBr, the scattering coefficients increase, regardless of the tested wavelengths. It is known that greater phosphor concentrations can boost the amount of scattering centers, thus increasing the scattering coefficient. Regardless, if said concentration becomes immoderate, granule consolidation may occur, lessening the scattering proficiency.

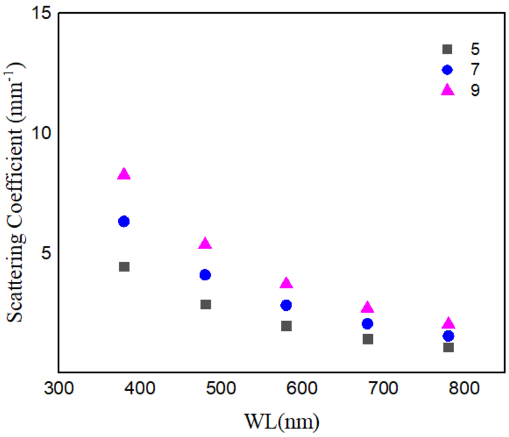

Fig. 1: The scattering coefficients with KBr at different concentrations

On the other hand, the longer the wavelength, the lower the scattering coefficients. Said finding indicate better scattering for shorter light, implying that the blue-pumped radiation can be absorbed by the phosphor for better light conversion. The lower scattering of longer-wavelengths light implies the probability of lower light trapping and better light extraction for lumen efficiency improvement. The increasing light scattering under higher concentrations of KBr can be contributed to the declining YAG:Ce^{3+} presence. As presented in Figure

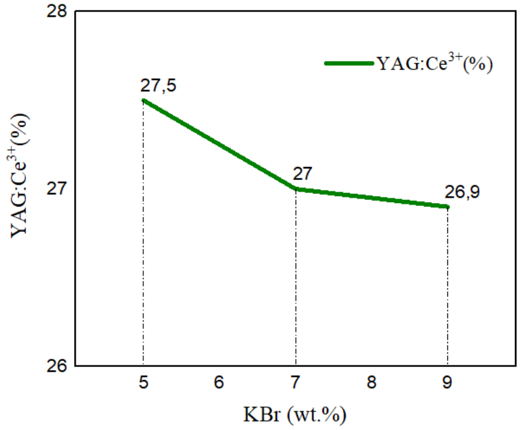

Fig. 2: The dosage of YAG:Ce^{3+} phosphor with KBr at different concentrations

2, the YAG:Ce^{3+} presence gradually decreases under growing KBr presence. The lower concentration of yellow phosphor can reduce the reabsorption by phosphor and the generation of heat by lost energy. As a result, the lumen output could be improved via increasing concentration of KBr.

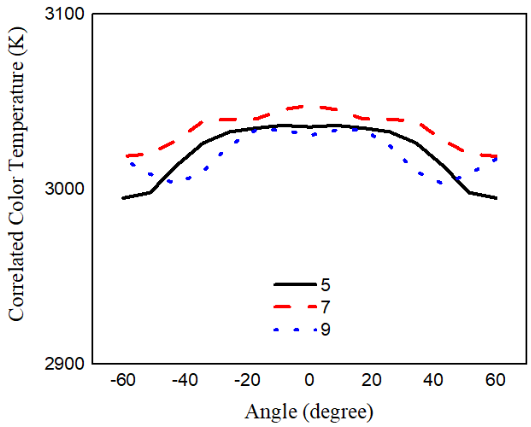

Fig. 3: The angular CCT with KBr at different concentrations

It is possible to notice the better color distribution across different angles with the scattering improvement. However, according to the data presented in Figure 3, a KBr concentration of 5 wt% exhibits a more uniform distribution in the tested angular range of $\pm 60°$. The

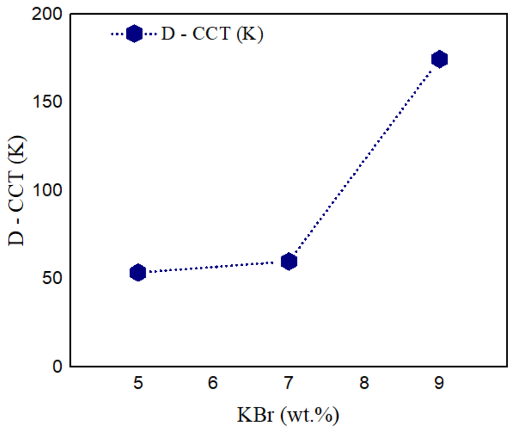

Fig. 4: The deviated angular CCT with KBr at different concentrations

higher concentration leads to the variations between different viewing angles. The fluctuation likely signifies higher CCT deviation. Figure 4 demonstrates the data of deviated CCT (D-CCT) with KBr concentrations of 5 wt%, 7 wt%, and 9 wt% in the phosphor film. An increase of 125 K in deviated CCT can be seen when the amount of KBr rises from 5 wt% to 9 wt%. In other words, concerning the testing scope of this simulation work, increasing KBr concentration does not benefit the uniformity of angular CCT.

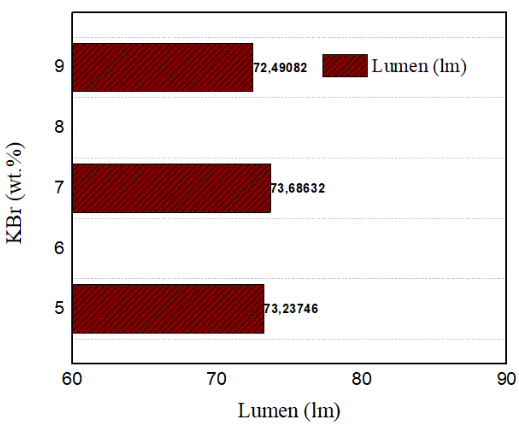

Fig. 5: The lumen output with KBr at different concentrations

In Figure 5, the lumen output is depicted with different doping amount of KBr. At 7 wt% KBr, the lumen output is the highest. Meanwhile, with KBr amount increasing to 9 wt%, the lumen declines and becomes even lower than the counterpart with 5 wt% KBr. The data shows that the fluctuation between lumen levels at three KBr concentrations is minor, resulting from the consistent luminescent properties of KBr. The thermal consistency of KBr can sustain proficiency under various temperature, lessening variance for illumination output. KBr is also proficient at energy transmutation when turning excitation power to form observable illumination [25, 26]. Notably, the increase of lumen strength with KBr positively suggest the potential of the material for improving the performance of WLED lumen efficiency.

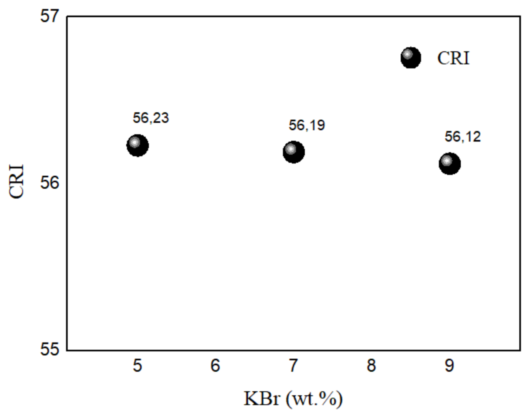

(a) CRI

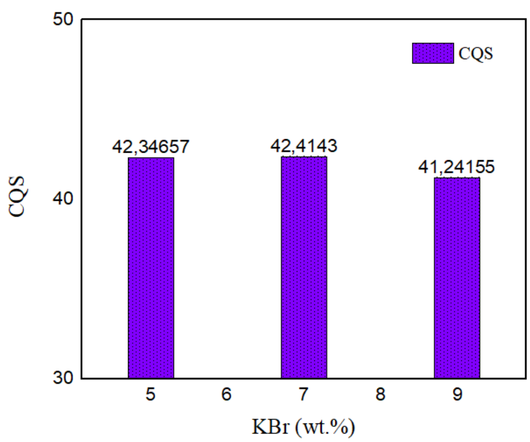

(b) CQS

Fig. 6: The rendering efficiency with KBr at different concentrations: (a) CRI and (b) CQS.

The color rendition of the WLED is presented in Figure 6. The concentration increase of KBr does not result in significant fluctuation in both color rendering index (CRI in Figure 6a) and color quality scale (CQS in Figure 6b). As seen in Figure 6a, CRI only shows consistent, but very negligible decreases as the KBr concentration increases. Concerning the data of KBr presence in the phosphor layer in Figure 6b, the CQS, unlike its counterpart CRI, is initially preserved when KBr amount increases to 7 wt%. A slight decline is only observed with higher KBr concentration of 9 wt%. Similar to the case of lumen mentioned above, such minor changes in CRI and CQS also results from the consistent luminescent properties of KBr, including thermal consistency as well as proficient energy transmutation. Therefore, in this simulation work, 5–7 wt% KBr is the optimal concentration for improvement in lumen output and color quality preservation.

The intention of CRI assessment is to validate the fidelity of a light source. However, in certain cases, a high-fidelity light source may not be optimal. For instance, in museum displays, some artworks have significantly faded over time. A high-fidelity source would accurately reproduce these faded colors without enhancement or restoration. Consequently, the values of these works of art would be underestimated. Therefore, more factors should be considered when reproducing color performance of a light source. Specifically, more color samples, including vivid colors, color saturation, color coordination, and user's preferences, need to be taken into consideration. In this situation, the CQS can be used as it is developed based on such factors.

4. Conclusion

In this study, simulations were conducted to explore the impact of incorporating KBr powder on conventional phosphor compounds, aiming to enhance the luminescence and color uniformity of white light-emitting diodes (WLEDs). The introduction of KBr powder, with an average radius of approximately 4 microns, is anticipated to induce scattering within the phosphor compound, thereby improving wide-angle light dispersion. Using Mie-Lorenz scattering theory and MATLAB® simulations, we varied the concentration of KBr powder in the phosphor mixture. The results indicate that increased concentrations of KBr powder lead to enhanced scattering strength; however, this also results in greater color deviation. A notable increase in lumen output was observed with KBr concentrations up to 7 wt%. Additionally, chromatic rendition performance remained relatively stable across different KBr concentrations. These findings suggest that KBr powder has the potential to improve the performance of phosphor compounds under visible excitation wavelengths, presenting a viable approach for optimizing WLED light output.

References

[1] L.-T. Chou, S.-H. Wu, H.-H. Hung, W.-Z. Lin, Z.-P. Chen, A. A. Ivanov, and S.-H. Chia. Compact multicolor two-photon fluorescence microscopy enabled by tailorable continuum generation from self-phase modulation and dispersive wave generation. *Opt. Express*, 30(22):40315, Oct 2022.

[2] Peter Fjodorow, Mikhail Frolov, Yuri Korostelin, Vladimir Kozlovsky, Christof Schulz, Stanislav Leonov, Yan Skasyrsky, and Nikolai Yuryshev. Intracavity absorption spectroscopy of hcl isotopes, h2o, ch4, c2h4, and c2h6 in the 3.1–3.4 µm spectral range using a cr:cdse laser. *Opt. Express*, 30(22):40347–40356, 10 2022.

[3] Cong Lv, Changjun Li, Kaida Xiao, and Cheng Gao. Interim connection space based on colorimetric values for spectral image compression and reproduction. *Opt. Express*, 30(22):40144–40160, Oct 2022.

[4] Yuan Li, Xu Shi, Liping Yang, Chunyu Pu, Qijuan Tan, Zhengchun Yang, and Hong Huang. Mc-gat: multi-layer collaborative generative adversarial transformer for cholangiocarcinoma classification from hyperspectral pathological images. *Biomed. Opt. Express*, 13(11):5794–5812, Nov 2022.

[5] K. Gaudfrin, J. Lopez, L. Gemini, M. Delaigue, C. Hönninger, R. Kling, and G. Duchateau. Fused silica ablation by double ultrashort laser pulses with dual wavelength and variable delays. *Opt. Express*, 30(22):40120–40135, Oct 2022.

[6] Hangchuan Zhang, Siyang Tu, Linshuang Li, Xingwu Chen, Yingming Zhao, Mingzhou Wu, Xin Zhang, Shengdong Zhang, and Lixuan Chen. Large scale transparency-adjustable mini-led display with recoverable color gamut by a highly transparent electrochromic shutter. *Opt. Express*, 30(22):39904–39910, Oct 2022.

[7] Qianni Li, Xinrong Xu, Yanbo Wu, De-Bin Zou, Yan Yin, and Yu Tong-Pu. Generation of single circularly polarized attosecond pulses from near-critical density plasma irradiated by a two-color co-rotating circularly polarized laser. *Opt. Express*, 30(22):40063–40074, 10 2022.

[8] Erik Förster, Daniela Stumpf, Lukas Werner, Hartmut Hillmer, and Robert Brunner. Hyperchromatic lens doublets with an extremely small equivalent abbe number employing diffractive elements and refractive materials with exceptional dispersion properties. *J. Opt. Soc. Am. A*, 39(11):1992–2000, 10 2022.

[9] Yunxuan Wei, Ming Zhao, and Zhenyu Yang. Silicon metasurface embedded fabry–perot cavity enables the high-quality transmission structural color. *Opt. Lett.*, 47(20):5344–5347, Oct 2022.

[10] Qi Lu, Yifan Ding, Wei Wang, Shijie Liu, and Min Xu. Vis-nir superachromatic triplet design with five-color correction for abroadband interferometer. *Appl. Opt.*, 61(30):8880–8888, Oct 2022.

[11] C. L. Bogh, A. J. Muhowski, M. D. Nelson, V. G. J. Rodgers, and J. P. Prineas. Measurement of recombination mechanisms in mid-infrared w-superlattices. *Opt. Mater. Express*, 12(11):4261–4267, Nov 2022.

[12] Yinger Zhang, Zhouyi Wu, Peiying Lin, Yang Pan, Yuting Wu, Liufang Zhang, and Jiangtao Huangfu. Hand gestures recognition in videos taken with a lensless camera. *Opt. Express*, 30(22):39520–39533, Oct 2022.

[13] Liquan Zhu, Binghui Yao, Linxiao Deng, Yuhua Yang, Guan Wang, Chun Gu, and Lixin Xu. Evaluation of gamut enhancement in yellow regions and a choice of optimal wavelength for a rgby four-primary laser display system. *Opt. Express*, 30(21):38938–38952, Oct 2022.

[14] Xiuwen Bi, Pengfei Wang, Tao Wu, Fusheng Zha, and Peng Xu. Non-uniform illumination underwater image enhancement via events and frame fusion. *Appl. Opt.*, 61(29):8826–8832, Oct 2022.

[15] Chen Fan, Hong Zhao, Zixin Zhao, Junxiang Li, Yijun Du, Xingyu Yang, and Lu Zhang. Single-shot quantitative phase imaging with phase modulation of a liquid crystal spatial light modulator (lc-slm) under white light illumination. *Opt. Lett.*, 47(20):5264–5267, Oct 2022.

[16] Gangyi Li, Yuan Liu, Qiwei Xu, Hao Liang, and Xihua Wang. Deep learning enabled inverse design of nanocrystal-based optical diffusers for efficient white led lighting. *Appl. Opt.*, 61(29):8783–8791, Oct 2022.

[17] Xinhao Wang, Yingchun Wu, Dongyan Xu, Botong Wen, Qimeng Lv, and Xuecheng Wu. Synthetic aperture rainbow refractometry. *Opt. Lett.*, 47(20):5272–5275, Oct 2022.

[18] Caixin Lin, Xiangwei Yi, Zhengxin Ji, Dandan Hou, and Yandan Lin. Optimum display luminance under a wide range of ambient light for cockpit displays. *Opt. Express*, 30(21):38439–38457, Oct 2022.

[19] Andrew-Hieu Nguyen, Khanh L. Ly, Charlotte Qiong Li, and Zhaoyang Wang. Single-shot 3d shape acquisition using a learning-based structured-light technique. *Appl. Opt.*, 61(29):8589–8599, Oct 2022.

[20] Liangfeng Chen, Zhongping Lee, Gong Lin, Yongchao Wang, Junwei Wang, and Wendian Lai. On the measurement of remote

sensing reflectance by a traditional above-water approach in small water bodies. *Appl. Opt.*, 61(29):8664–8670, Oct 2022.

[21] Jiurun Chen, Aiye Wang, An Pan, Guoan Zheng, Caiwen Ma, and Baoli Yao. Rapid full-color fourier ptychographic microscopy via spatially filtered color transfer. *Photon. Res.*, 10(10):2410–2421, Oct 2022.

[22] Chang Liu, Zhuocheng Zou, Yuan Miao, and Jun Qiu. Light field quality assessment based on aggregation learning of multiple visual features. *Opt. Express*, 30(21):38298–38318, Oct 2022.

[23] Anupa Kumari, Prakash Nayak, Bikash Patra, Krishnan Venkatasubbaiah, and Ritwick Das. Third-order nonlinear optical manifestations in an intramolecular proton transfer fluorophore due to tamm-plasmon based broadband optical absorbers. *J. Opt. Soc. Am. B*, 39(10):2857–2862, Oct 2022.

[24] Sen Lin, Penghui Sun, Hongwei Gao, and Zhaojie Ju. Haze optical-model-based nighttime image dehazing by modifying attenuation and atmospheric light. *J. Opt. Soc. Am. A*, 39(10):1893–1902, Oct 2022.

[25] Hao Liang, Gang Yang, Songchao Bai, Chao Li, Xueguo Li, Yinhua Wang, Jinshu Huang, Jun Ji, and Yongsheng Zhu. Efficient and tunable photoluminescence for terbium-doped rare-earth-based cs2naycl6 double perovskite. *Opt. Lett.*, 47(19):5176–5179, Oct 2022.

[26] Xuheng Cao, Yusheng Lian, Zilong Liu, Han Zhou, Bin Wang, Wan Zhang, and Beiqing Huang. Hyperspectral image super-resolution via a multi-stage scheme without employing spatial degradation. *Opt. Lett.*, 47(19):5184–5187, Oct 2022.

About Authors

Le Thi TRANG received a Master's degree in Information Technology from Lac Hong University, Vietnam, and is currently working as a lecturer at the Faculty of Information Technology, Dong Nai Technology University, Bien Hoa City, Vietnam. Her research interests include computer science, computer vision, image recognition and classification, face detection and recognition, abnormal motion detection, and graphic design. She can be contacted at email: lethitrang@dntu.edu.vn.

Nguyen Van DUNG received a Master's degree in mechanical engineering from the University of Technical Education, Ho Chi Minh City, Vietnam, and is currently working as a lecturer at the Faculty of Engineering, Dong Nai Technology University, Bien Hoa City, Vietnam. His research interests include system optimization techniques, simulation and modeling, machine design, mold design. He can be contacted at email: nguyenvandung@dntu.edu.vn.

